JOURNAL OF SOLID STATE CHEMISTRY **124,** 52–57 (1996)
ARTICLE NO. 0206

On the Crystallographic and Magnetic Structures of Nearly Stoichiometric Iron Monoxide

Helmer Fjellvåg, Fredrik Grønvold, and Svein Stølen[1]

Department of Chemistry, University of Oslo, P. O. Box 1033, N-0315 Oslo, Norway

and

Bjørn Hauback

Institute for Energy Technology, P. O. Box 40, N-2007 Kjeller, Norway

Received August 7, 1995; in revised form January 17, 1996; accepted February 29, 1996

Neutron diffraction experiments have been carried out at room temperature and at 12 K on a polycrystalline three-phase sample of nearly stoichiometric wüstite, magnetite, and iron (mole fractions 0.914, 0.080, and 0.006) in order to extend the structural description of wüstite to a region were defect clusters should be of less importance. The sample was prepared by controlled disproportionation of a quenched wüstite with composition $Fe_{0.9347}O$. Tetrahedral iron interstitials could not be substantiated from refinement of the room temperature diffraction pattern, hence showing that the number of defect clusters is small. The character of the magnetic order–disorder transition is significantly changed upon going from the highly non-stoichiometric regime to nearly stoichiometric FeO. The transition in near stoichiometric FeO is strongly cooperative. Two components of the low temperature antiferromangetic structure is extracted, the main component ($\mu_{\parallel} = 3.8(4)\ \mu_B$) is along the unique axis [111], while a second smaller ($\mu_{\perp} = 1.3(3)\ \mu_B$) is perpendicular to the unique axis.

INTRODUCTION

The structure of the grossly nonstoichiometric iron monoxide, wüstite, has been extensively studied. It is the classical example of a non-stoichiometric phase and exhibits an exceptionally complex defect structure. Wüstite is formed eutectoidally from iron and magnetite at around 843 K (1). It is highly defective, and the phase field does not, at least at atmospheric pressure, extend to stoichiometry (1). The iron content of the iron-rich phase boundary increases with temperature from the eutectoid composition $Fe_{\sim 0.932}O$ at 843 K to $Fe_{\sim 0.954}O$ at 1185 K. At higher temperatures exsolution of iron is observed (1). The phase is easily quenched and remains metastable at low temperatures for considerable periods of time.

The crystal structure was established as a highly defective form of the ideal NaCl-type structure by Wyckoff and Crittenden (2). The iron deficiency is associated with a predominance of vacancies in the Fe sublattice (3) which subsequently implies the formation of trivalent iron. A much more complex description of the defect structure has gradually matured. This development was initiated by the neutron diffraction study by Roth (4) which showed that some iron atoms occupy interstitial tetrahedra sites. This concept was further advanced by Koch and Cohen (5) who suggested vacancies and tetrahedral ions for form 13/4-clusters of 13 vacancies and four interstitial tetrahedral iron atoms. Aggregation of defects in form of larger clusters based on a smaller basic cluster was suggested from high temperature neutron diffraction by Cheetham *et al.* (6). The basic 4/1-cluster consists of a tetrahedrally coordinated iron atom surrounded by four additional vacancies at octahedral iron sites. A vacancy to interstitial ratio less than four is usually observed and is ascribed to corner and edge sharing of the 4/1-clusters. Different types of clusters is expected under any temperature and oxygen potential condition. The considerable short-range order reduces the zero-point entropy, which appears to be negligible in wüstite.

A phase transformation in quenched metastable wüstite at about 183 K was detected by low-temperature heat capacity measurements by Millar (7). Subsequent studies have shown this "anomaly" to be due an antiferro to paramagnetic transition (8, 9). The magnetic moments in the low-temperature phase are antiferromagnetically ordered perpendicular to the (111) plane. Below T_N, a deformation of the high-temperature cubic structure into a rhombohedral variant was observed by Toombs and Rooksby (10)

[1] To whom correspondence should be addressed.

0022-4596/96 $18.00

and Willis and Rooksby (11). The degree of deviation from cubic symmetry for the antiferromagnetic phase increases with increasing iron content (12) and with decreasing temperature (13).

The magnetic moments deduced from powder neutron diffraction results, from 2.36 to 3.27 μB (4, 12), are smaller than calculated by Kanamori, 4.4 μB, considering spin–orbit contributions (14). According to Roth (4), the small moment is due to paramagnetic islands associated with the defect complexes. The increase in T_N with increasing defect concentration reported by Koch and Fine (15) implies, however, according to Battle and Cheetham (12), that magnetic ordering occurs within and around the defect clusters—a fact which led Battle and Cheetham (12) to propose that the interstitial cations and the surrounding iron atoms are coupled by an antiferromagnetic exchange interaction. The spins in these regions are in the (111) plane and not along [111] as in the defect-free regions. This model is further supported by the observation of a field-enhanced magnetic susceptibility (16).

The present contribution relates to the structural and magnetic properties of wüstite approaching 1 : 1 stoichiometry and extends the structural description of wüstite to a region where defect clusters should be of less or even minor importance. An almost pure two-phase mixture of nearly stoichiometric wüstite and magnetite can be produced by careful disproportionation of quenched nonstoichiometric wüstites (17). Results from powder neutron diffraction studies at temperatures between 12 and 300 K are presented and discussed in relation to results from nonstoichiometric wüstite. The nearly stoichiometric iron monoxide is for practical reasons termed FeO throughout the paper. The two-phase mixture of FeO and Fe_3O_4 is for the same reason denoted FeO–Fe_3O_4.

EXPERIMENTAL

Sample Preparation

The nonstoichiometric wüstites used in this investigation were prepared from iron(III) oxide and iron. The Fe_2O_3 (pro analysi, E. Merck No. 3294) was heated in alumina boats in an electric furnace at 1070 K until constant mass was attained. This required about 40 h and resulted in a mass loss of 0.05%. According to analyses by the manufacturer and impurity limits are (in % by mass): Cl^-, 0.01, SO_4^{2-}, 0.01; N, Pb, Cu, Mg, Mn, Ni, Zn, 0.005; insoluble in HCl, 0.01. A spectrographic grade analysis showed in addition the presence of SiO_2, 50 ppm. A small part of the sample was reduced to pure metallic iron with dry hydrogen gas at 1120 K until the Fe_2O_3/Fe mass ratio was (1.4295 $\pm$ 0.0002), theoretically 1.4297. Mixtures of this iron and the Fe_2O_3 in the nominal Fe/O ratios 0.93 and 0.94 were heated in evacuated and sealed vitreous silica tubes at 1270 K for 2 days and cooled with the furnace. After crushing, the samples were reheated to 950 K for 3 days and quenched by dropping the samples into a water, ice, salt solution.

The oxygen content of the thus produced sample was determined by oxidation and reduction of 1.0–1.5 g samples at 1070 K in air or H_2, respectively, to constant mass in alumina boats. The resulting oxygen content in the samples corresponded to $Fe_{0.925}O$ and $Fe_{0.9374}O$. For further details see Grønvold *et al.* (18). The presently used two-phase sample of FeO and Fe_3O_4 was subsequently prepared by careful disproportionation of the $Fe_{0.9374}O$ sample in our adiabatic calorimeter, as described earlier (17, 19). Powder X-ray diffraction data were collected at 295 K with a Guinier–Hägg-type camera (Cr$K\alpha_1$ radiation, Si as internal standard (20)).

Neutron Diffraction

Powder neutron diffraction (PND) data were collected on the OPUS IV two-axis diffractometer at the JEEP II reactor, Kjeller, at and below room temperature. Cylindrical sample holders of aluminium or vanadium were used. Monochromatic neutrons of wavelength $\lambda = 182.5$ pm were obtained by reflection from the (111) planes of a germanium monochromator. The diffraction patterns were measured by means of five ^{3}He detectors, positioned 10° apart. Intensity data were collected from $2\Theta = 10$ to 100° in steps of $\Delta 2\Theta = 0.05°$. Intensity corrections owing to $\lambda/2$ and $\lambda/3$ contributions were made. Temperatures between 10 to 300 K were obtained by means of a Displex cooling system. A Lake Shore DRC 82C controller was used, and the temperature was measured and controlled by means of a silicon diode.

Structural and instrumental parameters were obtained from Rietveld-type profile refinements. The MPREP/MPROF versions (21) of the Rietveld program were used, allowing simultaneous refinements of three phases, all of which are magnetically ordered. Details of the refinements are discussed under results, section ii. Scattering amplitudes, b(Fe) = 9.540 and b(O) = 5.805 fm, were taken from Sears (22), whereas the magnetic form factors for Fe^{2+} and Fe^{3+} were taken from Watson and Freeman (23). Since the free-ion form factors were used, the results may differ slightly from those reported by Battle and Cheetham (12) who used form factors with 10% expansion along sin Θ/λ. Owing to the limited sin Θ/λ range, the modest resolution at high sin Θ/λ and the substantial correlation between temperature factors, occupation numbers and magnetic moments, comparative studies were performed also for a non-stoichiometric wüstite with composition $Fe_{0.925}O$.

RESULTS AND DISCUSSION

Phase Analysis

Nearly stoichiometric wüstite and magnetite are formed as an intermediate metastable two-phase mixture on heat-

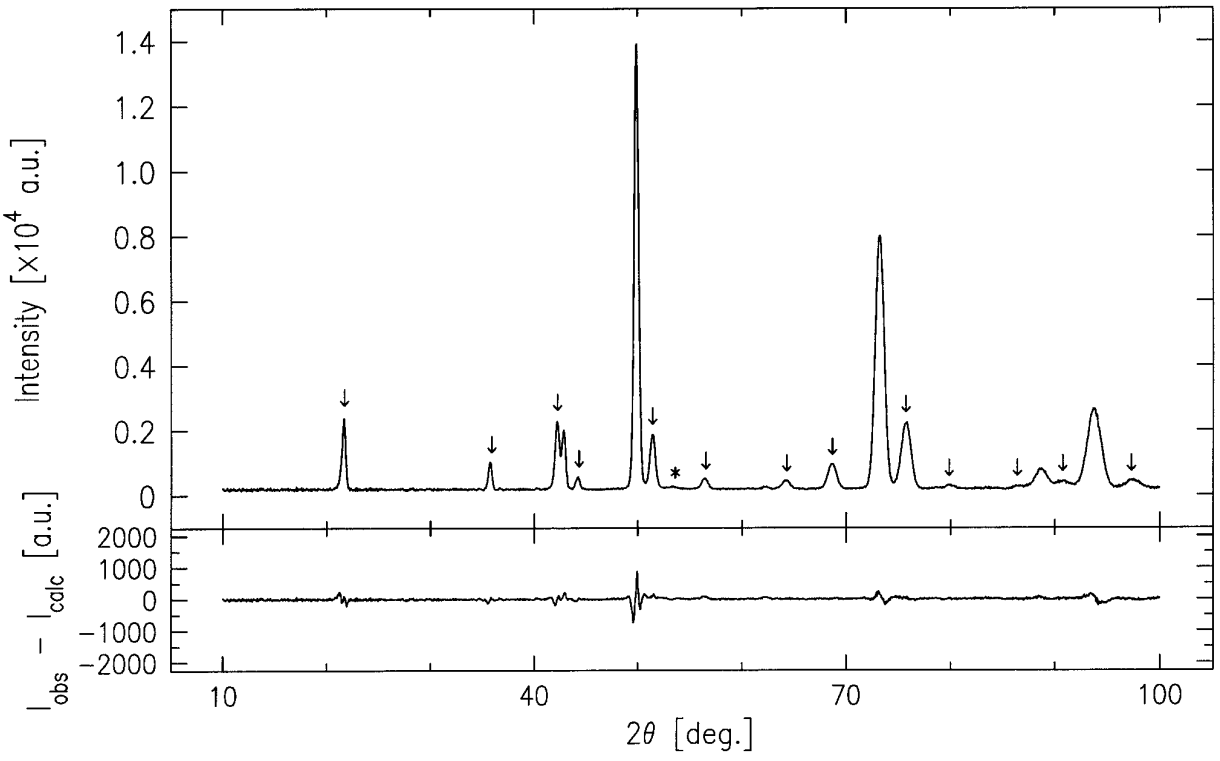

FIG. 1. Powder neutron diffraction pattern for the FeO–Fe_3O_4 sample at 298 K. Reflections from Fe_3O_4 marked with ↓, reflections from Fe with *; λ = 182.5 pm. Observed intensities and difference between observed and calculated intensities are shown.

ing rapidly quenched metastable wüstites. In a second disproportionation step, the stable two-phase mixture of iron and magnetite is formed (17, 19). For this reason, small amounts of iron may be present in the sample as both the exothermal disproportionation steps necessarily proceed with a finite speed even at very low temperatures. The powder neutron diffraction pattern at 298 K for the FeO–Fe_3O_4 sample is shown in Fig. 1. Only one faint iron-reflection is observed and the amount of iron in the sample is very small. The second disproportionation step, hence, proceeds very slowly below about 500 K. From the Rietveld type refinements (see below), individual scale factors were extracted for the three phases Fe, FeO, and Fe_3O_4. The amount of iron could be refined from room temperature data only where vanadium cylinders were used as sample containers since reflections from aluminium and iron overlap. Following the procedure described by Hill and Howard (24), the mole fractions of FeO and Fe_3O_4 and Fe are calculated as 0.914, 0.080, and 0.006. The deduced mole fractions are considered to be correct within an estimated uncertainty of ± 0.005 and are not significantly influenced by subtle changes in the defect description of FeO used during the different trial-refinements. The results are in good agreement with earlier estimates based on results from magnetization data (17, 19).

Crystallographic and Magnetic Structures at 298 K

For non-stoichiometric wüstite, the defect clusters consisting of vacancies at octahedral sites are situated around interstitial iron atoms (Fe^{III}) at tetrahedral sites of the cubic closed packed structure. The nature of these disordered clusters have been approached through theoretical calculations (25–27), and neutron diffraction/scattering studies. From the latter studies, the ratio between iron vacancies and interstitials (y/z) in wüstite, $Fe_x^{oct}\square_y^{oct}Fe_z^{tetr}O$, which contains information on the extension of the defect clusters, is obtained. The early studies by Roth (4) indicated a ratio around two (1.9 and 2.2 for $Fe_{0.945}O$ and $Fe_{0.926}O$); Battle and Cheetham (12) found higher values (2.78, 2.82 and 3.01 for $Fe_{0.943}O$, $Fe_{0.938}O$ and $Fe_{0.929}O$), whereas Garstein *et al.* (28) obtained intermediate values (2.55 and 2.56 for $Fe_{0.930}O$ and $Fe_{0.891}O$). Lattice energy calculations by Catlow and Fender indicate that the most stable small defect aggregates are formed by edge sharing rather than corner sharing of the basic 4/1-clusters giving preference to 6:2 and 8:3 clusters (25), i.e., to the vacancy to interstitial ratios 3.0 and 2.66. During the Rietveld-type refinements the occupation numbers for the octahedral and tetrahedral sites were refined, but constrained to match the overall composition of the sample. The obtained results

TABLE 1

Crystallographic and Magnetic Parameters Derived from Rietveld-Type Refinements of Powder Neutron Diffraction Data at 298 K for Single-Phase $Fe_{0.925}O$ and for the Three-Phase Mixture Containing FeO and Fe_3O_4, and a Small Amount of Fe

	$Fe_{0.925}O$	FeO	Fe_3O_4
a (pm)	430.64(1)	432.6(2)	840.45(4)
$n(Fe^{oct})$	0.870(3)[a]	1.00[b]	—
$n(Fe^{tetr})$	0.055[a]	0.00[b]	—
μ(Fe1)	—	—	3.78(8)
μ(Fe2)	—	—	3.84(16)
x(O)	—	—	0.2542(3)
R_p	4.5	9.8	
R_{exp}	4.3	5.4	

Note. For the rock-salt-type phase of $Fe_{0.925}O$ and FeO, space group *Fm-3m,* oxygen atoms in 4*b* positions, octahedral iron atoms (Fe^{oct}) in 4*a*, tetrahedral iron atoms (Fe^{tetr}) in 8*c*; for Fe_3O_4, spacegroup *Fd-3m*, Fe1 in 8a ($\frac{7}{8}$, $\frac{7}{8}$, $\frac{7}{8}$), Fe2 in 16*d* ($\frac{1}{2}$, $\frac{1}{2}$, $\frac{1}{2}$) and O in 32*e* (x, x, x). Calculated standard deviations in parentheses.

[a] Sum constrained to 0.0925.

[b] See text.

are given in Table 1. The present control experiments on $Fe_{0.925}O$ give $y/z = 2.4(1)$ in reasonable accordance with earlier studies. It should be noted that the defect ordering in wüstite is strongly dependent on thermal history, and some faint reflections in the powder neutron diffraction diagram indicate some longer range defect order as reported earlier (28).

One main aim of the Rietveld-type refinements was to obtain information about the defect situation for nearly stoichiometric FeO at 298 K. However, owing to the three-phase situation for the sample, the crystallographic and magnetic structure of magnetite at 298 K had to be refined simultaneously. Fe_3O_4 is of the inverse spinel type and is ferrimagnetically ordered at 298 K ($T_C \sim 850$ K) with antiferromagnetic coupling between atoms in octahedral and tetrahedral sites (29). In the Rietveld-type refinements, up to 18 variables were refined: three scale factors (FeO, Fe_3O_4 and Fe), two unit cell dimensions (FeO and Fe_3O_4), three half-width parameters, one instrumental zero point, one coordinate parameter (Fe_3O_4), two magnetic components (Fe_3O_4), and four temperature factors. In addition, occupation numbers for the octahedral and tetrahedral sites were refined in a similar way as described for $Fe_{0.925}O$. Since the exact composition of the iron monoxide phase is not definitely known, constrained refinements were carried out for different compositions (Fe_xO; $x = 1.000$, 0.995, 0.990, 0.985, 0.980). Judged from the reliability factors, the best fit was obtained for the model with no tetrahedral atoms. The difference between the different refinements is, however, very small and the exact stoichiometry of the nearly stoichiometric wüstite can not be determined from the present data since the limited sin Θ/λ range implies that the real uncertainty is probably larger than indicated by the calculated standard deviations. Still, the correct composition must be close to FeO. The composition deduced from the lattice constant, $Fe_{0.99}O$, is considered more reliable until significant evidences for another composition are obtained.

The presently obtained unit cell dimension for Fe_3O_4 at 298 K (see Table 1) indicates that magnetite in equilibrium with the nearly stoichiometric wüstite is iron-rich (19). The refined magnetic moments (Table 1) correspond to a total magnetic moment of 3.9(4) μB per Fe_3O_4 in good agreement with literature values (30, 31).

Crystallographic and Magnetic Structures at 12 K.

On cooling, FeO and $Fe_{0.925}O$ transform to a rhombohedrally distorted variant. The character of the transition is dramatically changed on going from the highly nonstoichiometric regime to nearly stoichiometric FeO as is reflected in the heat capacity in the transitional temperature range; see Fig. 2. Studies of the temperature dependence of the integrated intensity of selected reflections in the powder neutron diffraction pattern show that the additional magnetic scattering decreased smoothly toward zero on approaching $T_N = 197 \pm 5$ K (Fig. 3). The Brillouin function corresponding to $S = 2$ is included in the figure as a solid curve. The variation of the intensity of the selected reflections signalizes that the magnetic phase transition exhibits higher order characteristics in agreement with the calorimetric results which, however, gave a slightly lower Néel temperature. The transition in the nearly stoichiometric FeO has a much stronger cooperative character than the transitions in the nonstoichiometric wüstites.

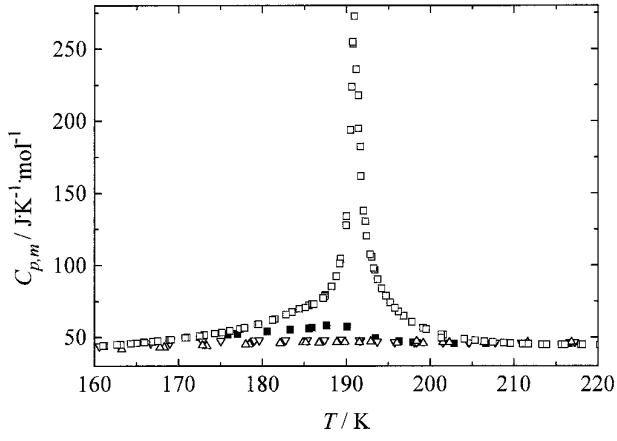

FIG. 2. Heat capacity of $Fe_{1-x}O$ near T_N. Results for $Fe_{0.99}O$ (□), $Fe_{0.947}O$ (■), $Fe_{0.9379}O$ (∇) and $Fe_{0.9254}O$ (Δ) are taken from Refs. (19, 32, 18, 18), respectively.

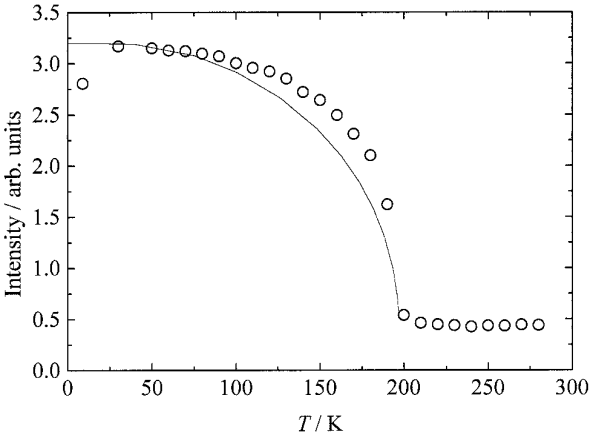

FIG. 3. Integrated intensity for the magnetic (1, 1, 1) reflection as function of temperature for FeO. The solid line represents the Brillouin function with $S = 2$.

The rhombohedral distortion of the unit cell of FeO is larger than in the non-stoichiometric wüstites. At 12 K, $a = 613.2(3)$ pm and $\alpha = 59.34(3)°$, whereas for the most iron rich wüstite earlier studied, $Fe_{0.943}O$, Battle and Cheetham (12) reported $a = 610.6(3)$ pm and $\alpha = 59.48(2)°$. In the refinements of the data at 12 K, the occupation numbers for the tetrahedral and octahedral sites were set to the values deduced at 298 K. For FeO, this implies that all octahedral sites were considered filled and no atoms at tetrahedral sites. The rhombohedral structures were described in space group $R\bar{3}$. For $Fe_{0.925}O$, the 16 interstitial sites for tetrahedral iron atoms in eight sets of 2*c*-positions ($x, x, x; \bar{x}, \bar{x}, \bar{x}$) were related by F-centering as is the case for the high-temperature phase and in accordance with earlier studies. Only one (common) x-parameter was refined. Finally, the magnetic structure of the iron monoxide had to be included in the refinements. According to Shull *et al.* (8) and Battle and Cheetham (12) the spins of the Fe^{2+} ions are ordered antiferromagnetically within (111) planes, their moments lying parallel to [111]. Neighboring planes have opposite spin directions so that the magnetic cell is twice as large as the chemical unit cell. In addition to the main component along [111] ($\mu_\parallel$) a smaller component perpendicular to [111] ($\mu_\perp$) is indicated by the present observation of the magnetic (111); (111) is observed both for FeO and for $Fe_{0.925}O$ but is stronger for the nearly stoichiometric compound (see $\mu_\perp$ in Table 2). The reason for the lacking $\mu_\perp$ in Battle and Cheetham's work is not understood. Several weak reflections presently observed for $Fe_{0.925}O$ suggest some degree of long range ordering of the defect clusters which may influence the magnetic structure to some degree. The observed large increase in the ordered magnetic moment, from 3.24(6) for $Fe_{0.925}O$

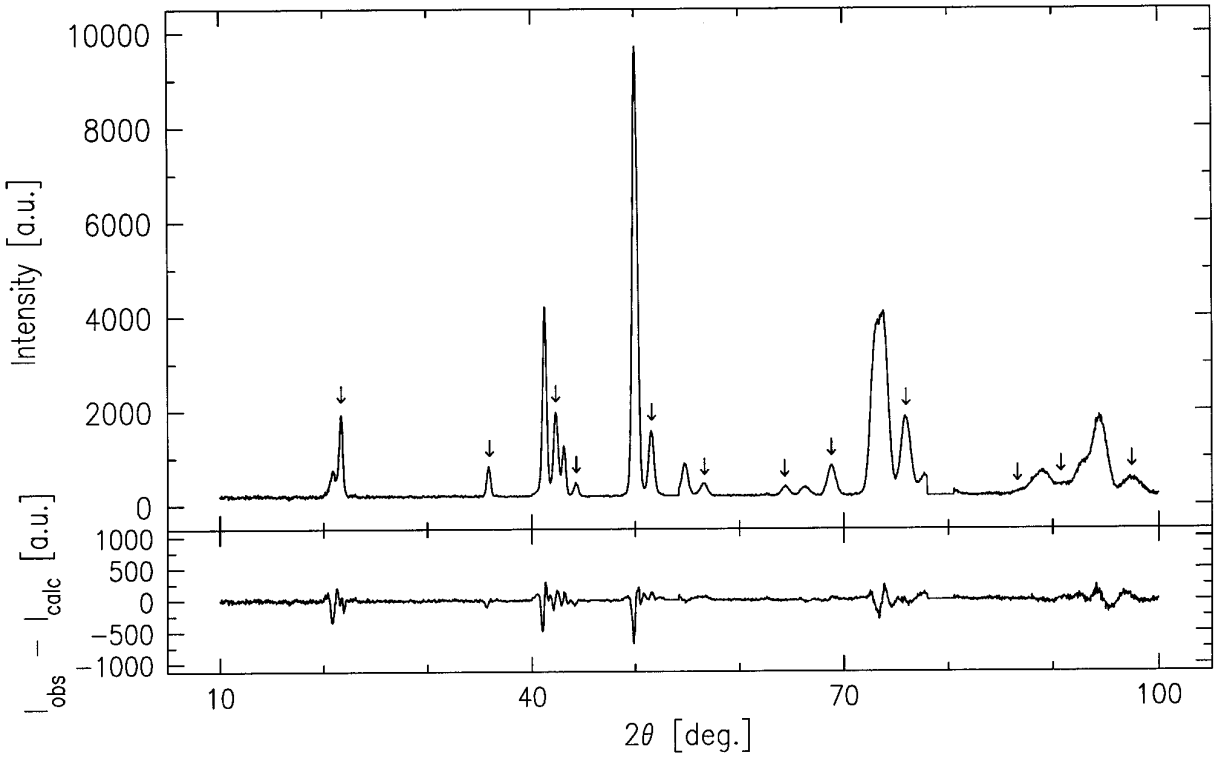

FIG. 4. Powder neutron diffraction pattern for the FeO–Fe_3O_4 sample at 12 K. Reflections from Fe_3O_4 marked with ↓; $\lambda = 182.5$ pm. Observed intensities and difference between observed and calculated intensities are shown.

TABLE 2

Crystallographic and Magnetic Parameters Derived from Rietveld-Type Refinements of Powder Neutron Diffraction Data at 12 K for Single-Phase $Fe_{0.925}O$ and for the Three-Phase Mixture Containing FeO, Fe_3O_4, and a Small Amount of Fe

	$Fe_{0.925}O$	FeO	Fe_3O_4
a (pm)	607.3(4)	613.2(3)	838.73(4)
α (°)	59.92(3)	59.34(3)	—
x(O)	—	—	0.2547(3)
$\mu(Fe_{\perp})$	0.70(2)	1.3(3)	—
$\mu(Fe_{\parallel})$	2.79(1)	3.8(4)	—
μ(Fe1)	—	—	4.23(8)
μ(Fe2)	—	—	3.80(18)
R_p	7.7	9.0	
R_{exp}	6.0	5.9	

Note. For the rock-salt-type phase of $Fe_{0.925}O$ and FeO, space group $R\bar{3}$, oxygen atoms in 2*c* (x, x, x) with $x = \frac{1}{4}$ (fixed) and 6*f* (x, y, z) with coordinates fixed to ($\frac{1}{4}$, $\frac{1}{4}$, $\frac{3}{4}$) positions, octahedral iron atoms (Fe^{oct}) in 1*a* (0, 0, 0), 1*b* ($\frac{1}{2}$, $\frac{1}{2}$, $\frac{1}{2}$), 3*d* ($\frac{1}{2}$, 0, 0), and 3*e* (0, $\frac{1}{2}$, $\frac{1}{2}$), tetrahedral iron atoms (Fe^{tetr}) in two 2*c*-positions (x, x, x) with coordinates repectively fixed to ($\frac{1}{8}$, $\frac{1}{8}$, $\frac{1}{8}$) and ($\frac{5}{8}$, $\frac{5}{8}$, $\frac{5}{8}$) and two 6*f*-positions (x, y, z) with coordinates, respectively, fixed to ($\frac{1}{8}$, $\frac{5}{8}$, $\frac{5}{8}$) and ($\frac{5}{8}$, $\frac{1}{8}$, $\frac{1}{8}$); for Fe_3O_4, spacegroup *Fd-3m*, Fe1 in 8*a* ($\frac{7}{8}$, $\frac{7}{8}$, $\frac{7}{8}$), Fe2 in 16*d* ($\frac{1}{2}$, $\frac{1}{2}$, $\frac{1}{2}$), and O in 32*e* (x, x, x). Calculated standard deviations in parentheses. Occupation numbers were fixed to values given in Table 1.

to 4.6(5) μ_B for FeO is closely related to a change in the defect structure. The presently obtained magnetic moment, for $Fe_{0.925}O$ is somewhat larger than those obtained by Roth (2.96 and 2.36 μ_B for $Fe_{0.945}O$ and $Fe_{0.926}O$) (4) but in agreement with Battle and Cheetham (3.27, 2.98 and 3.01 μ_B for $Fe_{0.943}O$, $Fe_{0.938}O$ and $Fe_{0.929}O$) (12). The value derived for FeO is close to the ideal magnetic moment 4.4 μ_B calculated by Kanamori (14) considering spin-orbit contributions. The low magnetic moments observed for the nonstoichiometric wüstites presumably (4, 12) arise from the presence of disordered islands of defect clusters in an antiferromagnetically ordered matrix. According to Battle and Cheetham (12), the closest iron neighbors arrange antiferromagnetically with respect to tetrahedral iron atoms. The magnetic clusters thereby formed are, however, disordered with respect to each other and to the overall antiferromagnetic order of the octahedral sublattice. This model has gained additional support from the observation of substantially increased magnetic moments on alignment in magnetic fields (16). The presently observed high magnetic moment for the nearly stoichiometric FeO is in agreement with expectations as the concentration of defect clusters in this case should be very small. It is thus concluded that FeO undergoes a strongly cooperative transition into a strongly rhombohedrally distorted phase with high magnetic moments and nearly perfect antiferromagnetic order. Still, the entropy of the cooperative part of the transition obtained from calorimetic studies (19) is somewhat lower than expected from spin-only considerations. Significant contributions to the disordering is, hence, expected both at low temperatures (below 100 K) and at high temperatures (above 300 K).

The presently obtained total magnetic moment 3.4(5) μB per Fe_3O_4 is reasonable taking the large standard deviation due to the small amount of magnetite in the sample into consideration.

REFERENCES

1. L. S. Darken and R. W. Gurry, *J. Am. Chem. Soc.* **67,** 1398 (1945).
2. R. G. W. Wycoff and E. D. Crittenden, *J. Am. Chem. Soc.* **47,** 2876 (1925).
3. E. R. Jette and F. Foote, *J. Phys. Chem.* **1,** 29 (1933).
4. W. L. Roth, *Acta Crystallogr.* **13,** 140 (1960).
5. F. Koch and J. B. Cohen, *Acta Crystallogr. Sect. B* **25,** 275 (1969).
6. A. K. Cheetham, B. E. F. Fender, and R. I. Taylor, *J. Phys. C: Solid State Phys.* **4,** 2160 (1971).
7. R. W. Millar, *J. Am. Chem. Soc.* **51,** 215 (1929).
8. C. G. Shull, W. A. Strauser, and E. O. Wollan, *Phys. Rev.* **83,** 333 (1951).
9. H. Bizette and B. Tzai, *C. R. Acad. Sci. Paris* **217,** 390 (1943).
10. N. C. Toombs and H. P. Rooksby, *Nature* **165,** 442 (1950).
11. B. T. M. Willis and H. P. Rooksby, *Acta Crystallogr.* **6,** 827 (1953).
12. P. D. Battle and A. K. Cheetham, *J. Phys. C: Solid State Phys.* **12,** 337 (1979).
13. Y. Suzuki, N. Kawai, and E. Asada, *Rep. Gov. Chem. Ind. Res. Inst. Tokyo* **60,** 375 (1965).
14. J. Kanamori, *Prog. Theor. Phys.* **17,** 177 (1957).
15. F. B. Koch and M. E. Fine, *J. Appl. Phys.* **38,** 1470 (1967).
16. M. S. Seehra and G. Srinivasan, *J. Phys. C* **17,** 883 (1984).
17. S. Stølen, R. Glöckner, and F. Grønvold, *Thermochim. Acta.* **256,** 91 (1995).
18. F. Grønvold, S. Stølen, P. Tolmach, and E. F. Westrum, Jr., *J. Chem. Thermodyn.* **25,** 1089 (1993).
19. S. Stølen, R. Glöckner, F. Grønvold, T. Atake, and S. Izumisawa, *Am. Mineral*, in press.
20. R. D. Deslattes and A. Henins, *Phys. Rev. Lett.* **31,** 972 (1973).
21. M. W. Thomas and P. J. Bendall, *Acta Crystallogr. Sect. A.* **34,** 351 (1978).
22. W. F. Sears, *Neutron News* **3**(3), 26 (1992).
23. R. E. Watson and A. J. Freeman, *Acta Crystallogr.* **14,** 27 (1961).
24. R. J. Hill and C. J. Howard, *J. Appl. Crystallogr.* **20,** 467 (1987).
25. C. R. A. Catlow and B. E. F. Fender, *J. Phys. C: Solid State Phys.* **8,** 3267 (1975).
26. A. B. Anderson, R. W. Grimes, and A. H. Heuser, *J. Solid State Chem.* **53,** 353 (1984).
27. M. R. Press and D. E. Ellis, *Phys. Rev. B* **35,** 4438 (1987).
28. E. Garstein, T. O. Mason, and J. B. Cohen, *J. Phys. Chem. Solids* **47,** 759 (1987).
29. C. G. Shull, E. O. Vollan, and W. C. Koehler, *Phys. Rev.* **84,** 912 (1951).
30. P. Weiss and R. Forrer, *Ann. Phys.* **12,** 279 (1929).
31. Z. Kakol and J. M. Honig, *Phys. Rev. B* **40,** 9090 (1989).
32. S. S. Todd and K. R. Bonnickson, *J. Am. Chem. Soc.* **73,** 3894 (1951).